

Important Notice to Authors

Attached is a PDF proof of your forthcoming article in PRB. Your article has 6 pages and the Accession Code is **BR12269**.

Please note that as part of the production process, APS converts all articles, regardless of their original source, into standardized XML that in turn is used to create the PDF and online versions of the article as well as to populate third-party systems such as Portico, CrossRef, and Web of Science. We share our authors' high expectations for the fidelity of the conversion into XML and for the accuracy and appearance of the final, formatted PDF. This process works exceptionally well for the vast majority of articles; however, please check carefully all key elements of your PDF proof, particularly any equations or tables.

Figures submitted electronically as separate PostScript files containing color usually appear in color in the online journal. However, all figures will appear as grayscale images in the print journal unless the color figure charges have been paid in advance, in accordance with our policy for color in print (<http://publish.aps.org/authors/color-figures-print>) and the relevant figure captions read "Color". For figures that will be color online but grayscale in print, please ensure that the text and captions clearly describe the figures to readers who view the article only in grayscale.

No further publication processing will occur until we receive your response to this proof.

Specific Questions and Comments to Address for This Paper

- 1 PRB prefers not to make claims of novelty or priority. Please check edits.
- 2 Please align numbers by decimal.
- 3 Please verify page no. in Ref. [10].
- 4 Please remove duplicate entry (i.e., Refs. [11] and [13]) from the reference list and renumber all subsequent reference citations in both the text and in the reference list.
- 5 Please check Ref. [12] for accuracy.
- 6 Please update all eprints with traditional published journal references, if possible.
- 7 Please check journal title in Ref. [16] for accuracy.

Other Items to Check

- Please note that the original manuscript has been converted to XML prior to the creation of the PDF proof, as described above. Please carefully check all key elements of the paper, particularly the equations and tabular data.
- Please check PACS numbers. More information on PACS numbers is available online at <http://publish.aps.org/PACS/>.
- Title: Please check; be mindful that the title may have been changed during the peer review process.
- Author list: Please make sure all authors are presented, in the appropriate order, and that all names are spelled correctly.
- Please make sure you have inserted a byline footnote containing the email address for the corresponding author, if desired. Please note that this is not inserted automatically by this journal.
- Affiliations: Please check to be sure the institution names are spelled correctly and attributed to the appropriate author(s).
- Receipt date: Please confirm accuracy.
- Acknowledgments: Please be sure to appropriately acknowledge all funding sources.
- Hyphenation: Please note hyphens may have been inserted in word pairs that function as adjectives when they occur before a noun, as in "x-ray diffraction," "4-mm-long gas cell," and "R-matrix theory." However, hyphens are deleted from word pairs when they are not used as adjectives before nouns, as in "emission by x rays," "was 4 mm in length," and "the R matrix is tested."

Note also that Physical Review follows U.S. English guidelines in that hyphens are not used after prefixes or before suffixes: superresolution, quasiequilibrium, nanoprecipitates, resonancelike, clockwise.

- Please check that your figures are accurate and sized properly. Make sure all labeling is sufficiently legible. Figure quality in this proof is representative of the quality to be used in the online journal. To achieve manageable file size for online delivery, some compression and downsampling of figures may have occurred. Fine details may have become somewhat fuzzy, especially in color figures. The print journal uses files of higher resolution and therefore details may be sharper in print. Figures to be published in color online will appear in color on these proofs if viewed on a color monitor or printed on a color printer.
- *Overall, please proofread the entire article very carefully.*

Ways to Respond

- **Web:** If you accessed this proof online, follow the instructions on the web page to submit corrections.
- **Email:** Send corrections to prbproofs@aptaracorp.com
Subject: **BR12269** proof corrections

- **Fax:** Return this proof with corrections to +1.703.791.1217. Write **Attention:** PRB Project Manager and the Article ID, **BR12269**, on the proof copy unless it is already printed on your proof printout.
- **Mail:** Return this proof with corrections to **Attention:** PRB Project Manager, Physical Review B, c/o Aptara, 3110 Fairview Park Drive, Suite #900, Falls Church, VA 22042-4534, USA.

Probing IrTe₂ crystal symmetry by polarized Raman scattering

N. Lazarević,¹ E. S. Bozin,² M. Šćepanović,¹ M. Opačić,¹ Hechang Lei (雷和畅),² C. Petrovic,² and Z. V. Popović¹

¹*Center for Solid State Physics and New Materials, Institute of Physics Belgrade, University of Belgrade, Pregrevica 118, 11080 Belgrade, Serbia*

²*Condensed Matter Physics and Materials Science Department, Brookhaven National Laboratory, Upton, New York 11973-5000, USA*

(Received 7 April 2014; revised manuscript received 26 May 2014; published xxxxxx)

Polarized Raman scattering measurements on IrTe₂ single crystals carried out over the 15–640 K temperature range, and across the structural phase transition, reveal different insights regarding the crystal symmetry. In the high temperature regime three Raman active modes are observed at all of the studied temperatures above the structural phase transition, rather than two as predicted by the factor group analysis for the assumed $P\bar{3}m1$ symmetry. This indicates that the actual symmetry of the high temperature phase is lower than previously thought. The observation of an additional E_g mode at high temperature can be explained by doubling of the original trigonal unit cell along the c axis and within the $P\bar{3}c1$ symmetry. In the low temperature regime (below 245 K) the other Raman modes appear as a consequence of the symmetry lowering phase transition and the corresponding increase of the primitive cell. All of the modes observed below the phase transition temperature can be assigned within the monoclinic crystal symmetry. The temperature dependence of the Raman active phonons in both phases is mainly driven by anharmonicity effects. The results call for reconsideration of the crystallographic phases of IrTe₂.

DOI: [10.1103/PhysRevB.00.004300](https://doi.org/10.1103/PhysRevB.00.004300)

PACS number(s): 78.30.-j, 74.25.Kc, 61.05.cp, 64.60.-i

I. INTRODUCTION

Although known for some time [1,2], the interest in IrTe₂ has been renewed recently with the discovery of superconductivity [3–6]. By doping this layered compound with Pt, Pd, and Cu, the phase transition which occurs at low temperatures [7] is suppressed and superconductivity emerges [3–6,8]. At room temperature IrTe₂ has a trigonal symmetry with edge-sharing IrTe₆ octahedra forming layers stacked along the c axis [7], as shown in Fig. 1. As temperature is decreased, the system undergoes a symmetry lowering phase transition in the temperature range between 220 and 280 K, with the exact transition temperature T_{PT} presumably depending on the sample form (powder versus single crystal) and the thermal cycle details (cooling or warming) [3–7,9]. The phase transition is accompanied by a hump in electrical resistivity and a drop in magnetic susceptibility [10], anomalies reminiscent of those associated with the onset of a charge-density-wave (CDW) state observed in other TX_2 systems [11]. However, the exact nature of the low temperature phase remains controversial, since no signatures of the CDW gap in IrTe₂ have been seen in angle resolved photoemission and optical spectroscopy studies [5,9,10]. Recent band structure calculations combined with x-ray absorption spectroscopy measurements suggest that the dramatic change in the interlayer and intralayer hybridizations could play an important role in the structural phase transition of IrTe₂ [6]. More recently, it has also been suggested that the depolymerization of the polymeric Te-Te bonds might be responsible for the structural phase transition [9].

Although prior crystallographic analyses showed that the IrTe₂ crystal structure changes from trigonal to monoclinic with decreasing temperature, the low temperature structure is still a subject of debate [7]. It was argued that the initially assigned monoclinic $C2/m$ symmetry cannot fully describe the structure below the phase transition [12–14]. Consequently, the proposed crystal symmetry was further lowered down to

triclinic $P\bar{1}$ [13] and even $P1$ [14]. Moreover, it was also suggested that the trigonal and monoclinic structures coexist intrinsically below the phase transition [12]. The nature of the phase transition as well as the symmetry of the low temperature phase therefore still remain open questions.

Important information concerning the symmetry of the crystal system can be obtained by utilizing the properties of Raman spectroscopy and by performing the measurements in different polarization configurations whereby one can probe different scattering channels. Raman spectroscopy also emerges as a valuable tool for detecting the intrinsic phase separation [15].

Here we present results of a systematic Raman scattering study on IrTe₂ single crystals. The spectra were collected in different scattering geometries at various temperatures. The room temperature Raman spectra were analyzed within the trigonal crystal symmetry. Three instead of two peaks, which are predicted by the factor group analysis (FGA) for the $P\bar{3}m1$ space group, are observed in the Raman spectra, suggesting a different crystal symmetry of IrTe₂ in the high temperature phase from that previously assumed. The same phonon structure persists at $T \gg T_{PT}$, indicating that it is a true characteristic of the high temperature phase. At temperatures below $T_{PT} = 245$ K, the clear fingerprint of the first order structural phase transition is observed in the Raman spectra. The observed modes are interpreted within the monoclinic crystal symmetry. No signatures of the trigonal unit cell presence have been detected in the low temperature Raman scattering spectra. All temperature induced effects in both phases are mostly anharmonic. These observations provide important insights and constraints for possible crystal symmetries of this system in different temperature regimes.

II. EXPERIMENT

Single crystals of IrTe₂ were prepared by the self-flux method. Ir and Te were mixed in an 18:82 stoichiometric

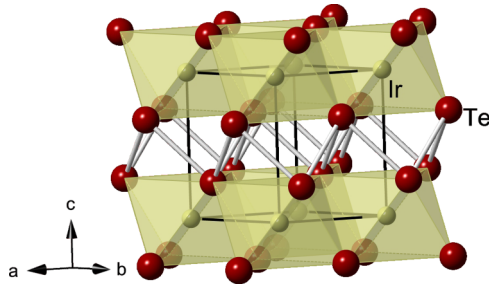


FIG. 1. (Color online) Crystal structure of IrTe₂ in the trigonal phase. Solid lines represent a single $P\bar{3}m1$ unit cell, with yellow (red) spheres indicating the positions of Ir (Te).

ratio, heated in alumina crucibles under an Ar atmosphere up to 1160 °C, kept at that temperature for 24 h, and then cooled to 400 °C over 130 h. Excess Te flux was removed at 400 °C by centrifugation. Platelike mm-size crystals were obtained. Magnetization and resistivity data were measured by warming the sample from 5 K. They are in good agreement with published values [3].

Raman scattering measurements were performed using a JY T64000 Raman system with 1800/1800/1800 grooves/mm gratings and a TriVista 557 Raman system with the 900/900/1800 grooves/mm gratings combination, both in a backscattering micro-Raman configuration. The 514.5 nm line of a mixed Ar⁺/Kr⁺ gas laser was used as an excitation source. High temperature measurements were performed in an Ar environment by using a Linkam THGS600 heating stage. Low temperature measurements were performed using a KONTI CryoVac continuous flow cryostat with a 0.5 mm thick window in the warming regime. Complementary atomic pair distribution function (PDF) measurements at 300 K were performed on a finely pulverized sample at the X17A beamline of the National Synchrotron Light Source (NSLS) at Brookhaven National Laboratory, utilizing a 67.42 keV x-ray beam within a commonly used rapid-acquisition setup [16] featuring a sample to detector distance of 204.25 mm, and with access to a wide momentum transfer range up to 28 Å⁻¹. Standard corrections, PDF-data processing, and structure modeling protocols were utilized, as described in detail elsewhere [17].

III. RESULTS AND DISCUSSION

IrTe₂ crystallizes in a trigonal type of structure ($P\bar{3}m1$ space group) with one molecular unit per unit cell (Fig. 1) [7,19]. The crystal structure consists of IrTe₂ layers which are made up of edge-sharing IrTe₆ octahedra. Short Te-Te bonds between adjacent IrTe₂ result in three-dimensional polymeric networks, thereby reducing the c/a ratio in comparison with the standard hexagonal closed packing of the CdI₂ structure [1,9,20]. This is related to the Ir⁺³ state and the fractional oxidation state of Te anions (Te^{-1.5}) [2,9].

A. High temperature phase

Figure 2 shows the room temperature polarized Raman scattering spectra of IrTe₂ single crystals measured from the (001) plane of the sample. Although the FGA for the

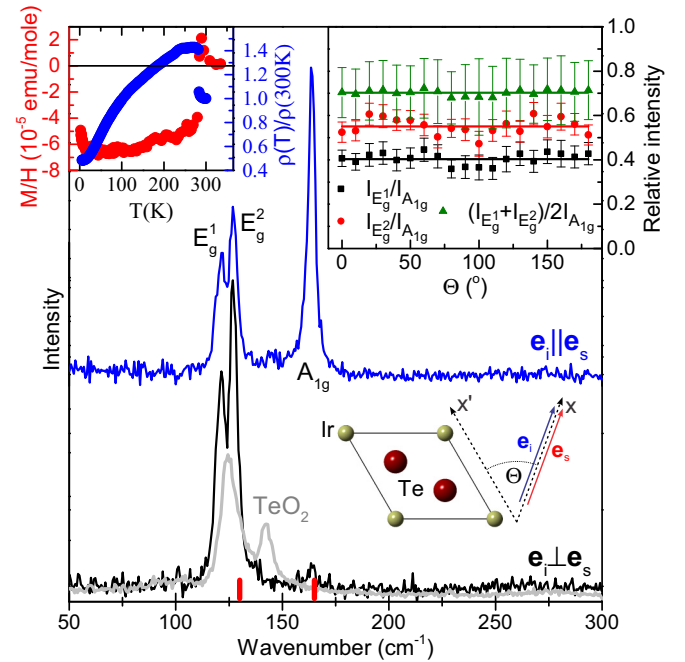


FIG. 2. (Color online) Room temperature Raman scattering spectra of IrTe₂ measured using a JY T64000 Raman system in different polarization configurations. Gray lines represent the spectra of TeO₂ with scaled intensity. Red markers represent phonon energies at Γ point calculated by Cao *et al.* [11]. Inset on the left: Magnetization and resistivity data measured by warming the sample from the base temperature. Inset on the right: Relative intensities of the Raman active modes measured in a parallel polarization configuration for different orientations of the sample with respect to the laboratory axis.

$P\bar{3}m1$ space group predicts only two Raman active modes ($A_{1g} + E_g$) to be observed in the scattering experiment, three peaks are clearly distinguished in the data. A contribution to the Raman spectra originating from scattering on possible TeO₂ impurities can be safely excluded (see Fig. 2). According to the selection rules for the trigonal system, summarized in Table I, the A_{1g} mode can only be observed in a parallel but not in a crossed polarization configuration, whereas the E_g mode can be observed in both parallel and crossed polarization configurations. Consequently, the peak at about 164 cm⁻¹, which is indeed observed in a parallel but not in a cross polarization configuration, is attributed to the A_{1g} symmetry mode. The energy of this mode is in very good agreement with the calculated value [11] (red mark in Fig. 2). Whereas the numerical calculations [11] further predict a single E_g mode at about 130 cm⁻¹ to be observed in the Raman scattering experiment, two peaks at about 121 and 126 cm⁻¹ are unambiguously observed in the data in this energy range (see Fig. 2). These modes are observed in both parallel and cross polarization configurations, which suggests their E_g symmetry. The appearance of two modes in the energy range where only one mode is expected indicates that the original crystal symmetry assignment for the high temperature phase may be inadequate, and that the actual symmetry is in fact lower. We consider the issue of the symmetry of the high temperature phase in more detail next.

TABLE I. Considerations of Raman tensors for three different crystal systems and the Raman mode distribution in the Γ point and various space groups of interest for IrTe₂.

Crystal system	Raman tensors [18]		Raman modes
Trigonal ($O_z \parallel C_3$ $O_y \parallel C_2$)	$\hat{R}_{A_{1g}} = \begin{pmatrix} a & 0 & 0 \\ 0 & a & 0 \\ 0 & 0 & b \end{pmatrix}$	$\hat{R}_{E_g} = \begin{pmatrix} -c & 0 & 0 \\ 0 & c & 0 \\ 0 & 0 & 0 \end{pmatrix}, \begin{pmatrix} 0 & c & 0 \\ c & 0 & 0 \\ 0 & 0 & 0 \end{pmatrix}$	$\Gamma_{P\bar{3}m1} = A_{1g} + E_g$ $\Gamma_{P\bar{3}c1} = A_{1g} + A_{2g}(\text{silent}) + 2E_g$
Monoclinic ($O_y \parallel C_2$)	$\hat{R}_{A_g} = \begin{pmatrix} b & 0 & d \\ 0 & c & 0 \\ d & 0 & a \end{pmatrix}$	$\hat{R}_{B_g} = \begin{pmatrix} 0 & f & 0 \\ f & 0 & e \\ 0 & e & 0 \end{pmatrix}$	$\Gamma_{C2/m} = 2A_g + B_g$
Triclinic	$\hat{R}_A = \hat{R}_{A_g} = \begin{pmatrix} a & d & e \\ d & b & f \\ e & f & c \end{pmatrix}$		$\Gamma_{P\bar{1}} = 21A_g$ $\Gamma_{P1} = 222A$

The first possibility is that the IrTe₂ symmetry is lowered at room temperature to some t subgroup of the $P\bar{3}m1$ [21]. This would imply splitting of a double degenerate E_g mode into an A_g - B_g doublet [22]. Hereby the obtained modes would display different angular Raman intensity dependencies as the sample orientation is varied in a parallel polarization configuration (see Fig. 2). On the contrary (as can be seen in the inset of Fig. 2), both modes at 121 and 126 cm⁻¹ exhibit the same angular intensity dependence, thereby excluding the possibility of the E_g mode splitting, i.e., symmetry lowering to some t subgroup of the $P\bar{3}m1$. Furthermore, it confirms the E_g nature of the 121 and 126 cm⁻¹ modes since, for a trigonal system (see Table I), both A_{1g} and E_g mode intensities are independent on the sample orientation when measured in a parallel polarization configuration.

The second possibility which could explain the observed appearance of the two E_g modes instead of a single E_g mode is the symmetry change to some k subgroup of $P\bar{3}m1$ [21]. The simplest option is $P\bar{3}c1$ ($Z = 2$) with Ir atoms located on the $2b$ site and Te atoms at the $4d$ site. The $P\bar{3}c1$ unit cell is built by doubling of the $P\bar{3}m1$ unit cell along the c axis (see Fig. 1). The FGA for the $P\bar{3}c1$ predicts three Raman active modes to be observed in the Raman scattering experiment ($A_{1g} + 2E_g$), which is in complete agreement with our findings. To further verify the plausibility of this assumption, we performed a structural analysis of room temperature x-ray PDF data of IrTe₂ using the $P\bar{3}c1$ model. The fit results are shown in Fig. 3 and summarized in Table II.

Importantly, the observed phonon structure and, consequently, the crystal $P\bar{3}c1$ symmetry persist at temperatures

$T \gg T_{PT}$ deep in the high temperature regime, as is evident from Fig. 4, indicating that these are the characteristics of the high temperature phase. As the temperature is increased, all of the modes are shifted toward lower energies and become progressively broader (see the inset of Fig. 4). All of the changes of the spectra induced by a temperature increase are in accordance with the well known anharmonicity model [23–25].

B. Low temperature phase

By lowering the temperature, IrTe₂ undergoes the phase transition in the range between 220 and 280 K [7,13,14]. The origins of the phase transition as well as the crystal symmetries of IrTe₂ at low temperatures are still under vigorous debate [7,12–14].

Polarized Raman scattering spectra of IrTe₂ measured at low temperatures (between 15 and 300 K) in parallel and cross polarization configurations are presented in Fig. 5. Significant changes in the spectra in both polarization configurations are observed around 245 K. A lower transition temperature is a consequence of the local heating effects of the sample by the laser beam. Unlike in the case of a canonical CDW phase transition where additional modes gradually appear [26], the observed sudden change in the phonon spectra suggests the first order character of the phase transition. The existence of at least 11 peaks in the low temperature phase indicates lowering of the symmetry and/or an increase of the unit cell size.

Figure 6 shows polarized Raman scattering spectra of IrTe₂ measured at 15 K in parallel and cross polarization configurations. A significant difference in the spectra measured in the parallel and crossed polarization configurations

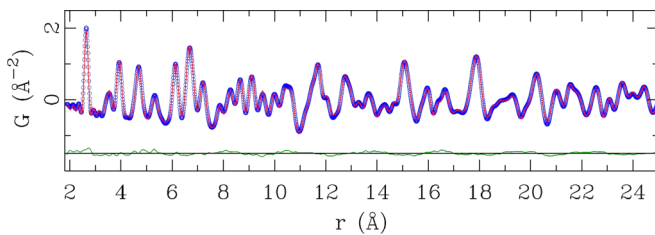


FIG. 3. (Color online) Room temperature x-ray PDF of IrTe₂: Experimental data (blue open symbols), $P\bar{3}c1$ model (red solid line), and difference curve (green solid line) which is offset for clarity. Structural parameters are summarized in Table II.

TABLE II. Structural parameters for the $P\bar{3}c1$ phase obtained from PDF analysis at 300 K. The lattice parameters are $a = b = 3.929(4)$ Å, $c = 10.805(2)$ Å. U_{ij} (Å² × 10³) are nonzero components of the displacement tensor.

Atom	x	y	z	$U_{11} = U_{22}$	U_{33}
Ir	0	0	0	6(2)	6(3)
Te	1/3	2/3	0.126(1)	7(2)	9(4)
$\chi^2 = 0.002$					
$R_{wp} = 0.106$					

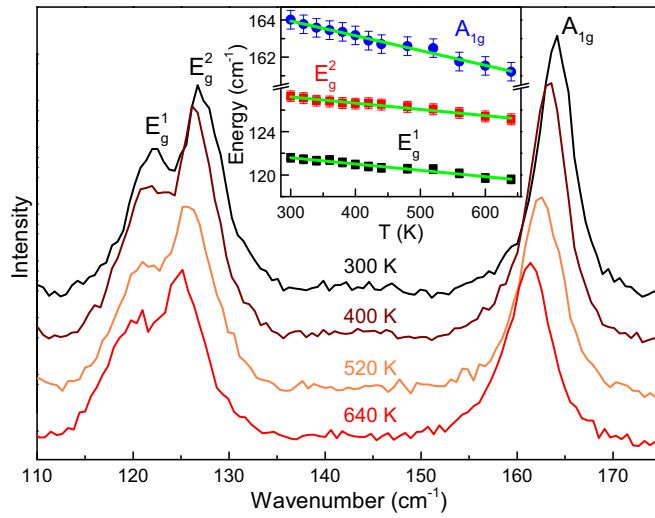


FIG. 4. (Color online) Raman scattering spectra of IrTe₂ single crystals measured at various temperatures, as indicated, in the high temperature regime using a TriVista 557 Raman system. Inset: Energy temperature dependence of the A_{1g} , E_g^1 , and E_g^2 Raman active modes. The solid green lines represent calculated spectra by using the standard three-phonon anharmonicity model [23], where $[\omega_0 = 123.4(2) \text{ cm}^{-1}, C = 0.26(2) \text{ cm}^{-1}]$, $[\omega_0 = 129.0(2) \text{ cm}^{-1}, C = 0.27(2) \text{ cm}^{-1}]$, and $[\omega_0 = 160.4(2) \text{ cm}^{-1}, C = 0.48(3) \text{ cm}^{-1}]$ are the best fit parameters for the E_g^1 , E_g^2 , and A_{1g} Raman active modes, respectively.

indicates the existence of the two separate scattering channels in the low temperature phase. Symmetry arguments suggest that in the case of the triclinic crystal structure only one channel can be observed. Due to the proposed orientation of the triclinic lattice [13,14] in relation to the trigonal lattice,

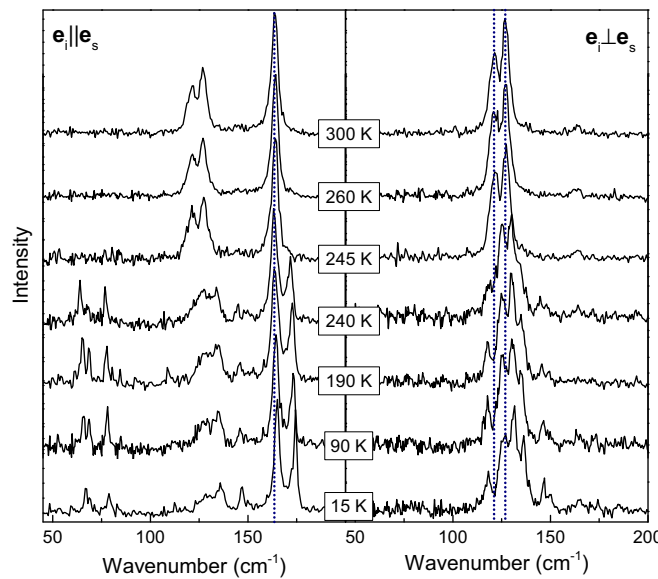


FIG. 5. (Color online) Polarized Raman scattering spectra of IrTe₂ measured at various temperatures, as indicated, in the low temperature regime using a JY T64000 Raman system in parallel and cross polarization configurations. The spectra were measured by warming the sample from 15 K. Dotted vertical lines represent a guide to the eyes.

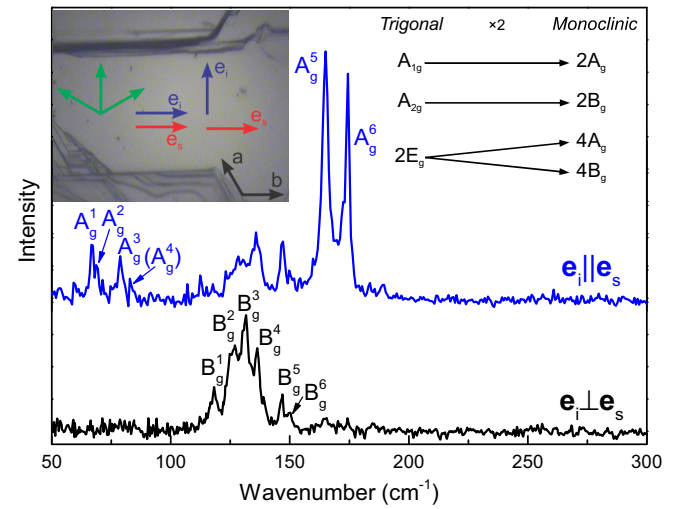


FIG. 6. (Color online) Polarized Raman scattering spectra of IrTe₂ measured at 15 K using a JY T64000 Raman system in parallel and cross polarization configurations. Inset on the left: Image of the IrTe₂ sample. Inset on the right: Correlation diagram connecting Raman active phonons for trigonal and monoclinic types of structures.

the contribution to the scattering intensity (in our scattering geometry) would come from nearly all the components of the Raman tensor (see Table I) and the cancellation of some Raman modes in different polarization configurations is highly unlikely. Furthermore, for both $P1$ and $P\bar{1}$ space groups, a substantially larger number of Raman modes is expected to be observed in the measured spectra. All this suggests that the IrTe₂ crystal symmetry in the low temperature phase should be higher than triclinic ($P1$ or $P\bar{1}$). The next crystal system with two different scattering channels is monoclinic (see Table I). The obtained spectra may be interpreted within the monoclinic crystal symmetry provided that the optical axis of the low temperature phase is orthogonal to the direction of incident light in the Raman scattering experiment, i.e., if it lies in the (001) plane of the trigonal phase. This is consistent with the picture proposed by Matsumoto *et al.* [7]. At this point one should have in mind that symmetry breaking may occur along three equivalent directions, as indicated by the green arrows in the left inset of Fig. 6. For generality we assume the contributions from all three possible orientations. Consequently, one may expect the appearance of the B_g modes in both parallel and cross polarization configurations. Although the A_g modes may be also observed in both parallel and cross polarization configurations (with the assumption of twinning), in the crossed polarization configuration the intensity of the A_g modes depends on the $|b - c|^2$ and the cancellation can be easily achieved.

Following the previous arguments, the peaks at about 67, 69, 79, 165, and 174 cm^{-1} which can be observed in parallel but not in cross polarization configurations may be assigned as the A_g symmetry modes. We believe that the weak structure at about 83 cm^{-1} may also be the A_g symmetry mode, however, very low intensity prevents unambiguous assignment. Six peaks at about 118, 126, 131, 136, 148, and 150 cm^{-1} that can be observed in both parallel and crossed polarization configurations are assigned as the B_g symmetry modes.

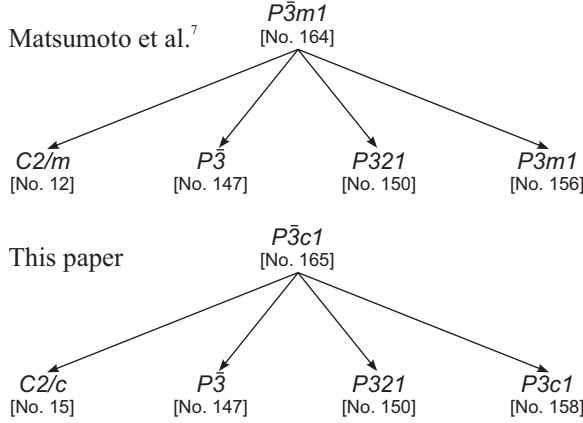


FIG. 7. Schematics of maximal nonisomorphic subgroup relations of the space group $P\bar{3}m1$ [7] (upper panel) and $P\bar{3}c1$ (lower panel) for the t subgroup. The number of the space group is given in the parentheses.

Although the properties of the observed Raman modes can, in principle, be interpreted within the monoclinic crystal system, the proposed [7] unit cell of the $C2/m$ symmetry group with $Z = 2$ cannot account for the number of observed Raman modes. According to FGA for $C2/m$ ($Z = 2$), only three modes are expected to be observed in the Raman scattering experiment (see Table I). Consequently, a larger unit cell within the monoclinic crystal system is needed to reproduce the observed Raman spectra. Following the previous arguments and the discussion regarding the symmetry of the high temperature phase, we may conclude that the space group symmetry of IrTe₂ at low temperatures should be searched for within the monoclinic $C2/c$ space group or some of its t subgroups (see Fig. 7) [21].

The temperature evolution of the Raman spectra (see Fig. 5) across the phase transition can be seen as the splitting of the two E_g modes into A_g (A_g^1 - A_g^4) and B_g (B_g^1 - B_g^4) quartets due to symmetry lowering and (at least) a two times increase of the primitive cell size (see the right inset in Fig. 6). The A_g^5 and A_g^6 most likely originate from the A_{1g} mode whereas the B_g^5 and B_g^6 originate from the A_{2g} mode of the trigonal phase. The absence of the E_g^1 and E_g^2 modes (within our experimental resolution), characteristic for the trigonal phase, in the low temperature Raman spectra of IrTe₂ suggests the absence of the trigonal lattice at low temperatures [12].

The temperature dependence of the energy and linewidth for the highest intensity Raman modes is shown in Fig. 8. A clear fingerprint of the first order phase transition is observed in both the energy and the linewidth of the observed modes. The solid lines represent the calculated spectra for the low temperature phase by using the three-phonon anharmonicity model [23]. Good agreement with the experimental data confirms that anharmonicity plays a major role in the temperature dependence of the temperature phase phonon self-energy below T_{PT} .

IV. CONCLUSION

A Raman scattering study of IrTe₂ single crystals has been presented. At room temperature, three instead of two

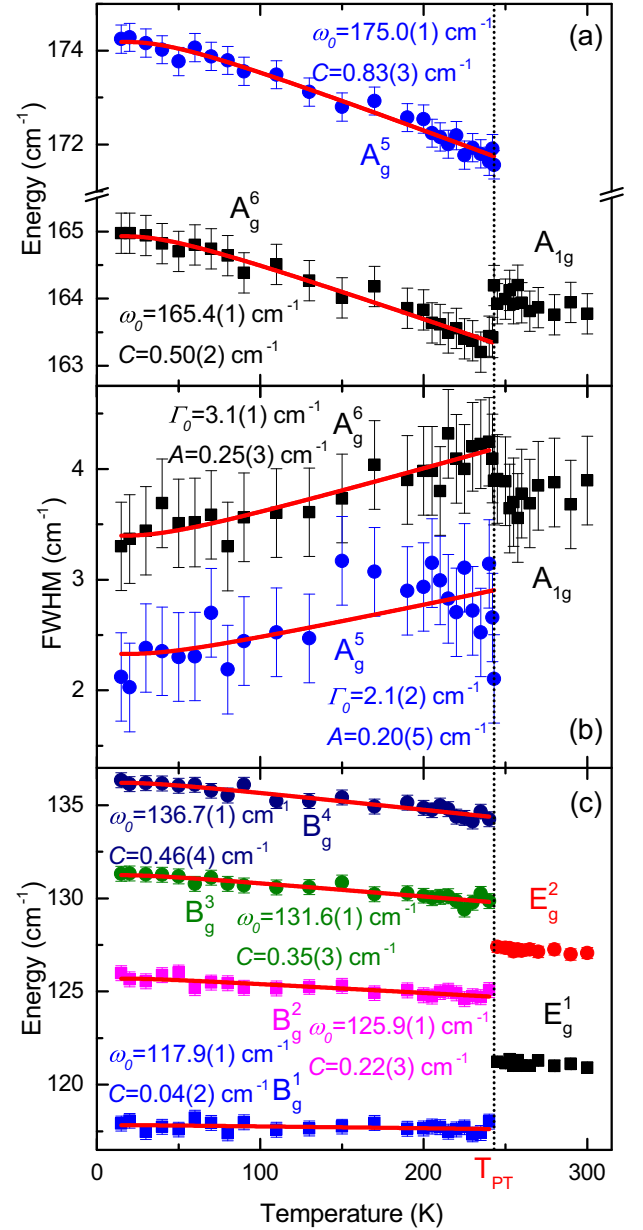


FIG. 8. (Color online) Temperature dependence of the highest intensity Raman mode energy (a) and (c) and linewidth (b). Solid lines represent the calculated spectra by using the standard three-phonon anharmonicity model [23]. The spectra were measured by warming the sample from 15 K.

Raman active modes predicted by the factor group analysis for the $P\bar{3}m1$ symmetry group are observed. The Raman data showed that the $P\bar{3}c1$ rather than the $P\bar{3}m1$ crystal symmetry is needed to describe the phonon structure of IrTe₂ at room temperature. The sudden change in the Raman spectra below $T_{PT} = 245$ K revealed the first order structural phase transition. The properties of the phonon spectra below T_{PT} are well interpreted within the monoclinic crystal symmetry. The splitting of the E_g modes at the T_{PT} comes from the symmetry lowering and the increase in the size of the unit cell. We believe that the space group symmetry of IrTe₂ at low temperatures should be searched for within the monoclinic $C2/c$ space group or some of its t subgroups. Further structural

investigations of both trigonal and monoclinic phases of IrTe₂ are needed. Apart from the symmetry change at T_{PT} , the temperature dependence of the energy and linewidth of the Raman active modes of IrTe₂ is mostly anharmonic.

ACKNOWLEDGMENTS

We gratefully acknowledge discussions with R. Hackl. This work was supported by the Serbian Ministry of Educa-

tion, Science and Technological Development under Projects No. ON171032 and No. III45018, as well as the Serbian-Germany bilateral project “Interplay of Fe-vacancy ordering and spin fluctuations in iron-based high temperature superconductors.” Part of this work was carried out at the Brookhaven National Laboratory which is, as well as the NSLS facility, operated for the Office of Basic Energy Sciences, US Department of Energy by Brookhaven Science Associates, under Contract No. DE-AC02-98CH10886.

-
- [1] S. Jobic, P. Deniard, R. Brec, J. Rouxel, A. Jouanneaux, and A. N. Fitch, *Z. Anorg. Allg. Chem.* **598**, 199 (1991).
 - [2] S. Jobic, R. Brec, and J. Rouxel, *J. Solid State Chem.* **96**, 169 (1992).
 - [3] J. J. Yang, Y. J. Choi, Y. S. Oh, A. Hogan, Y. Horibe, K. Kim, B. I. Min, and S.-W. Cheong, *Phys. Rev. Lett.* **108**, 116402 (2012).
 - [4] S. Pyon, K. Kudo, and M. Nohara, *J. Phys. Soc. Jpn.* **81**, 053701 (2012).
 - [5] D. Ootsuki, Y. Wakisaka, S. Pyon, K. Kudo, M. Nohara, M. Arita, H. Anzai, H. Namatame, M. Taniguchi, N. L. Saini, and T. Mizokawa, *Phys. Rev. B* **86**, 014519 (2012).
 - [6] M. Kamitani, M. S. Bahramy, R. Arita, S. Seki, T. Arima, Y. Tokura, and S. Ishiwata, *Phys. Rev. B* **87**, 180501 (2013).
 - [7] N. Matsumoto, K. Taniguchi, R. Endoh, H. Takano, and S. Nagata, *J. Low Temp. Phys.* **117**, 1129 (1999).
 - [8] A. Kiswandhi, J. S. Brooks, H. B. Cao, J. Q. Yan, D. Mandrus, Z. Jiang, and H. D. Zhou, *Phys. Rev. B* **87**, 121107 (2013).
 - [9] Y. S. Oh, J. J. Yang, Y. Horibe, and S.-W. Cheong, *Phys. Rev. Lett.* **110**, 127209 (2013).
 - [10] A. F. Fang, G. Xu, T. Dong, P. Zheng, and N. L. Wang, *Sci. Rep.* **3**, 1153 (2013).
 - [11] H. Cao, B. C. Chakoumakos, X. Chen, J. Yan, M. A. McGuire, H. Yang, R. Custelcean, H. Zhou, D. J. Singh, and D. Mandrus, *Phys. Rev. B* **88**, 115122 (2013).
 - [12] L. Zhang, X. Zhu, L. Ling, C. Zhang, L. Pi, and Y. Zhang, *Philos. Mag.* **94**, 439 (2014).
 - [13] H. Cao, B. C. Chakoumakos, X. Chen, J. Yan, M. A. McGuire, H. Yang, R. Custelcean, H. Zhou, D. J. Singh, and D. Mandrus, *Phys. Rev. B* **88**, 115122 (2013).
 - [14] G. L. Pascut, K. Haule, M. J. Gutmann, S. A. Barnett, A. Bombardi, S. Artyukhin, D. Vanderbilt, J. J. Yang, S.-W. Cheong, and V. Kiryukhin, [arXiv:1309.3548](https://arxiv.org/abs/1309.3548).
 - [15] N. Lazarević, M. Abeykoon, P. W. Stephens, H. Lei, E. S. Bozin, C. Petrovic, and Z. V. Popović, *Phys. Rev. B* **86**, 054503 (2012).
 - [16] P. J. Chupas, X. Qiu, J. C. Hanson, P. L. Lee, C. P. Grey, and S. J. L. Billinge, *J. Appl. Crystallogr.* **36**, 1342 (2003).
 - [17] T. Egami and S. J. L. Billinge, *Underneath the Bragg Peaks: Structural Analysis of Complex Materials*, 2nd ed. (Elsevier, Amsterdam, 2012).
 - [18] H. Kuzmany, *Solid-State Spectroscopy: An Introduction* (Springer, Berlin, 2009).
 - [19] C. Soulard, P. Petit, P. Deniard, M. Evain, S. Jobic, M.-H. Whangbo, and A.-C. Dhaussy, *J. Solid State Chem.* **178**, 2008 (2005).
 - [20] E. Canadell, S. Jobic, R. Brec, J. Rouxel, and M.-H. Whangbo, *J. Solid State Chem.* **99**, 189 (1992).
 - [21] T. Hahn, U. Shmueli, A. A. J. C. Wilson, and E. Prince, *International Tables for Crystallography* (Reidel, Dordrecht, 2005).
 - [22] W. G. Fateley, F. R. Dollish, N. T. McDevitt, and F. F. Bentley, *Infrared and Raman Selection Rules for Molecular and Lattice Vibrations: The Correlation Method* (Wiley-Interscience, New York, 1972).
 - [23] M. Balkanski, R. F. Wallis, and E. Haro, *Phys. Rev. B* **28**, 1928 (1983).
 - [24] N. Lazarević, Z. V. Popović, R. Hu, and C. Petrovic, *Phys. Rev. B* **81**, 144302 (2010).
 - [25] N. Lazarević, M. Radonjić, M. Šćepanović, H. Lei, D. Tanasković, C. Petrovic, and Z. V. Popović, *Phys. Rev. B* **87**, 144305 (2013).
 - [26] N. Lazarević, Z. V. Popović, R. Hu, and C. Petrovic, *Phys. Rev. B* **83**, 024302 (2011).